KINETICS OF CATHODIC PENETRATION OF ALUMINUM INTO NICKEL

M. E. Niyazimbetov, I. I. Astakhov, and B. N. Kabanov

UDC 541.138.3-034.71

Electrochemical penetration has been studied at room temperature to determine its mechanism, its contribution to the electrochemistry of aqueous and nonaqueous solutions [1], and as a quantitative means for deriving its kinetics [2]. Where rates of penetration into an electrode are diffusion limited, quantitative correlation of theory and experiment is greatly hampered by room temperature boundary diffusion and metastable phase formation. Comparisons are further complicated by almost complete absence of studies on diffusion in metallic systems near room temperature.

Electrochemical penetration from the molten state is associated with equilibrium phase formation so that diffusion rates of the penetrating element become large enough to be readily measured and compared with literature data.

We selected an aluminum–nickel system for study. Notwithstanding its complexity, physical metallurgists have devoted much attention to this system. Electrochemists are also quite familiar with nickel aluminides as the source of Raney nickel catalyst. The system is known to have four intermediate phases [4]: Ni_3Al (homogeneous region at 600°C contains 23 to 27.5 at.% Al), NiAl (40 to 55 at.% Al), Ni_2Al_3 (59.2 to 67.3 at.% Al), and $NiAl_3$ with a very narrow region of homogeneity.

Electrochemical studies were carried out with a $KCl-AlCl_3$ melt (1 : 1) at 600 ± 1°C in a sealed quartz cell. The cell was first evacuated and then filled with purified argon. Special purity, nonaqueous salts were used to prepare the electrolytes. An argon-filled, sealed chamber containing the salts was placed into the cell. Working electrodes were type NP-2 nickel sheets with a thickness of 0.2 mm and an area of 1 cm^2, previously annealed at 900°C in a hydrogen atmosphere for 8 h. The auxiliary electrode was a hollow cyclinder of type A-999 aluminum with the working electrode in the center. Chronopotentiometric and chronoamperometric measurements were made with a P-5848 potentiostat; x-ray phase studies were carried out with a URS-50I apparatus, and electron diffraction patterns were taken with UÉMF-100K electron microscope, All potentials were measured against an aluminum reference electrode placed in the same melt. In our experiments, the open circuit potential of the nickel electrode was 0.95 V and could be maintained at this value for several hours. Potentials at which various nickel aluminides are formed were determined through chronopotentiometric, x-ray phase, and electron diffraction studies.

Figure 1 displays an anodic chronopotentiogram of a nickel electrode with prior cathodic polarization at $\varphi = 0.0$ V. The four potential arrests indicate the presence of at least four different phases* that are situated at the following potentials: I) 0.1 to 0.2 V; II) 0.40 to 0.45 V; III) 0.5 to 0.6 V; and IV) 0.7 V to the open-circuit potential of nickel. We first polarized the electrodes cathodically at various fixed potentials for 1 to 5 h and studied the structures of the phases thus formed. As a rule, lines for more than one compound were found in x-ray diffraction patterns of electrodes polarized at potentials of 0.05 to 0.48 V. This is because the x-ray method provides information on the phase composition of electrode surface layers several microns thick. These may consist of sequential films, of intermetallic compounds such as are formed through reactive diffusion. Composition of the external intermetallic compound, richest in aluminum, is of interest in the study of penetration kinetics. We therefore took reflectance electron diffraction patterns of electrodes cathodically polarized for 1 h. A comparison of the three methods indicates that arrest IV corresponds to decomposition of a solid solution of Al in Ni; arrest III, to that of Ni_3Al; arrest II, to that of NiAl; and arrest I, to that of Ni_2Al_3. The aluminide $NiAl_3$ occurs on the electrode only after polarization at potentials 20-30 mV more negative than

* Conclusions should not be drawn on the amount of a particular phase from the length of an anodic arrest.

Institute of Electrochemistry, Academy of Sciences of the USSR, Moscow. Translated from Élektrokhimiya, Vol. 14, No. 6, pp. 930-934, June, 1968. Original article submitted June 20, 1977.

0038-5387/78/1406-0799$07.50

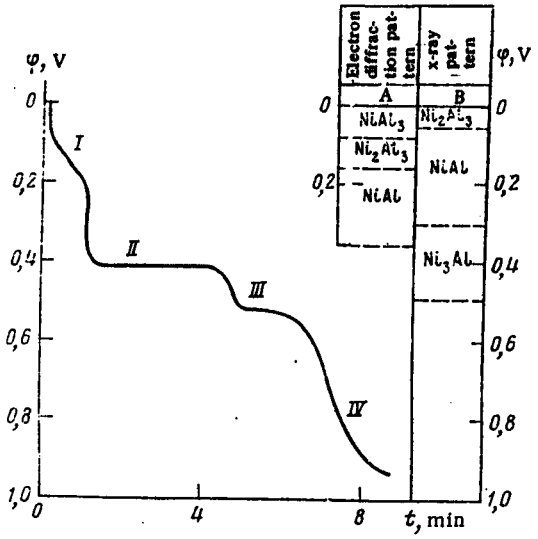

Fig. 1. Anodic chronopotentiogram (I-IV) of a nickel electrode with prior cathodic polarization for 5 min at 0 V; $i_a = 16$ mA/cm^2, T = 600° C. Relation of surface layer composition to penetration potential: A) Phase on the electrode surface (electron diffraction pattern); B) phase richest in aluminum, as detected through x-ray diffraction.

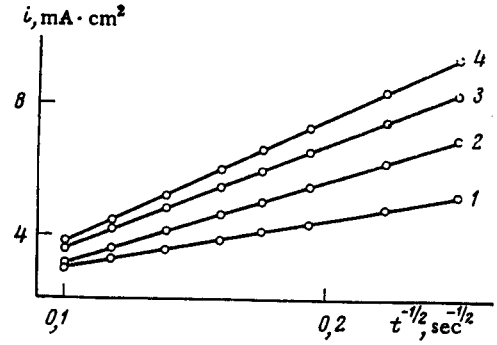

Fig. 2. Relation of penetration current to time at various φ (V): 1) 0.15; 2) 0.13; 3) 0.11; 4) 0.09.

that at the beginning of initial arrest I. An arrest corresponding to decomposition of this aluminide was not observed on our chronopotentiogram because of the thinness of the layer.

Penetration kinetics was studied by cathodic chronoamperometry. After obtaining an i, t curve for the potential φ_1, the electrode was held at a more positive potential φ_0 until the current became very small. We than applied a potential φ_2, usually more negative than φ_1, plotted the i,t curve for this potential, again held the electrode at φ_0, etc. We selected a φ_0 to correspond with the initial potential range for the formation of a particular phase, it was 0.52 V for studying the formation kinetics of Ni_3Al, NiAl, and Ni_2Al_3.

Current drop curvatures were straightened in i vs $t^{-1/2}$ coordinates, as shown in Fig. 2. Penetration of aluminum into nickel is thus diffusion limited and obeys the laws

$$i = Kt^{-1/2}, \qquad (1)$$

in which bulk rather than boundary diffusion plays the leading role [5]. Average diffusion coefficients as a function of phase composition were found to be 10^{-10} to 10^{-13} cm$^2 \cdot$ sec^{-1}, which are characteristic of diffusion in

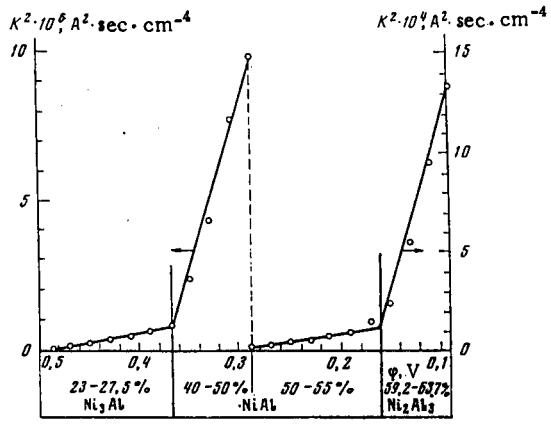

Fig. 3. Relation of K to penetration potential. $\varphi_0 = 0.52$ V; concentration is given in atomic percent of aluminum.

various aluminides at 600°C. We calculated K values of the penetration rates for each potential, making use of the slopes of the linear i vs $t^{-1/2}$ curves [6].

The kinetics of electrochemical penetration [7] has been based on the generally accepted concept of the linearity of irreversible thermodynamics, i.e., that the magnitude of driving forces is proportional to current:

$$J = LX, \tag{2}$$

where L is a coefficient. A penetrating element is characterized by a chemical potential gradient when its entry rate into a thickening layer of intermetallic compound is diffusion limited and when various forces are in equilibrium on the electrode surface. Substitution of concentration gradient by chemical potential gradient in the diffusion equation enabled us to disregard the effect of concentration on the diffusion coefficient. The effect can be marked in compounds with highly interreactive components, even at relatively small concentration changes.

Nevertheless, the coefficient L in Eq. (2) is generally dependent on the diffusant concentration and this relation is stronger the greater the concentration change. We may therefore expect that Eq. (2) will actually be more exact the narrower the homogeneous region of the intermetallic compound and the stronger the interreaction between its components. Applicability of the theory to an actual case where a compound is formed with a narrow homogeneous region has been demonstrated for the penetration of lead into platinum from molten salts to form a PtPb compound [6].

Figure 3 shows the relation we found between K (from Eq. (1)) and potential in coordinates of K^2 vs φ. It is evident that K rises with an increase in negative electrode potential and that K^2 varies linearly with potential in regions where each compound is formed [6]. Two sections with different slopes are observed in the potential region corresponding to the formation of NiAl. This may be due to a change in diffusion mechanism when NiAl passes through a concentration corresponding to exact stoichiometry (50 at.% Al) [8]. As regards diffusion, we have here two apparently individual compounds: one between 40 and 50 at. % Al and the other between 50 and 55 at. % Al. As expected, the choice of φ_0 markedly affects the absolute values of K but has no influence on the nature of the relation of K to potential. The relation of K^2 to potential is evidence that Ni_3Al, NiAl, and Ni_2Al_3 fulfill the linearity requirement of Eq. (2) with regard to current and driving forces.

The theory [7] is consequently also applicable to those cases where penetration causes the formation of compounds with a comparatively wide homogeneous region, i.e., up to 10 at.%. This is most likely where the selected system is characterized by considerable deviation from ideality. For example, a change in equilibrium potential from 0.29 to 0.16 V, i.e., 0.13 V, corresponds to a concentration change of aluminum in NiAl of only 5% (from 50 to 55 at.%) but a change in the activity coefficient of approximately 200 times. The data in Fig. 3 shows that the penetration rate under these conditions varies by approximately a factor of 3.5.

LITERATURE CITED

1. B. N. Kabanov, I. G. Kiseleva, and I. I. Astakhov, Élektrokhimiya, 8, 955 (1972).
2. B. N. Kabanov, I. G. Kiseleva, I. I. Astakhov, N. N. Tomashov, and P. I. Petukhova, Élektrokhimiya, 10, 765 (1974).
3. I. G. Kiseleva, Élektrokhimiya, 3, 275 (1967).
4. M. Hansen and K. Anderko, Structures of Binary Alloys [in Russian], Metallurgiya, Moscow (1962).
5. G. Schwitzgebel, Z. Phys. Chem. (Leipzig), 99, 217 (1976).
6. A. I. Fomichev and N. G. Chovnyk, Élektrokhimiya, 10, 284 (1974).
7. I. I. Astakhov, Élektrokhimiya, 9, 521 (1973).
8. G. W. Goward and D. H. Boone, Oxid. Met., 3, 475 (1971).

THE DIFFUSE ELECTRIC DOUBLE LAYER IN THE ADSORPTION OF ω-AMINOENANTHIC ACID ON MERCURY

B. B. Damaskin and Yu. N. Kuryakov

UDC 541.135.5-183:547

Under conditions in which the adsorption of an organic compound is localized within the dense portion of the double layer and does not disturb the equipotentiality of the outer Helmholt surface, the capacitance of the double layer is described well by the model of Grahame [1] as shown in our earlier work [2, 3]. A breakdown in the equipotentiality of the outer Helmholt surface and a corresponding deviation from the Grahame model was found in our previous work on the adsorption of a series of organic compounds which form condensed films on mercury [4]. As noted in our previous work [5], a breakdown in the Grahame model may also be expected for the adsorption of large dipolar organic molecules which partially extend into the diffuse layer and disturb the structure of this layer. In particular, sufficiently long ω-amino acids which form zwitterions in aqueous solutions with very considerable dipole moments should have these properties [6]. The adsorption behavior of ω-aminocaproic and ω-aminoenanthic acids at the solution/mercury and solution/air phase boundaries was studied in our previous work [7, 8]. The purpose of the present work was the investigation of the effect of ω-aminoenanthic acid (ω-AEA) on the structure of the diffuse portion of the electric double layer.

The differential capacitance of a mercury dropping electrode was measured using a P-568 alternating-current bridge. The electrocapillary curves were taken using an electrometer with a U-shaped water-proofed capillary [9, 10]. The samples of sodium fluoride and ω-AEA were subjected to careful purification by two- and threefold recrystallization from doubly distilled water.

In Fig. 1, differential capacitance curves (C, E curves) in solutions of 0.1 M ω-AEA on the background of 0.1, 0.03, 0.01, and $5 \cdot 10^{-4}$ M NaF were presented. As seen from this figure, at background concentration 0.03 M, a minimum appears on the C,E curves which deepens with increasing dilution of the background electrolyte, which indicates the diffuse nature of this minimum. However, the minimum of the C,E curves is at 0.33 V more positive than the zero-charge potential ($E_{q=0}$) which was found from electrocapillary measurements (see Fig. 2). Thus, as might have been expected, the adsorption of ω-AEA leads to a significant rearrangement of the diffuse layer and calculation of the capacitance according to the Grahame model leads to a significant discrepancy with the experimental C,E curve (see curves 1 and 2 on Fig. 3).

The strong shift in the minimum on the C,E curves towards more positive values relative to $E_{q=0}$ may be explained on the assumption that the $-CO_2^-$ group which forms the negative end of the ω-AEA zwitterion is located in the dense layer, whereas the $-NH_3^+$ group extends into the diffuse layer. In light of electroneutrality

$$q + q_1 = -q_2, \tag{1}$$

where q_1 is the charge of "specifically adsorbed" $-CO_2^-$ groups and q_2 is the total charge of the diffuse layer including the positive charges of the zwitterions. As shown by a calculation based on the Gibbs equation and

M. V. Lomonosov Moscow State University. Translated from Élektrokhimiya, Vol. 14, No. 6, pp. 934-936, June, 1978. Original article submitted June 21, 1977.

0038-5387/78/1406-0802$07.50